

# RSY-1 Is a Local Inhibitor of Presynaptic Assembly in *C. elegans*

Maulik R. Patel<sup>1</sup> and Kang Shen<sup>1,2,3\*</sup>

As fundamental units of neuronal communication, chemical synapses are composed of presynaptic and postsynaptic specializations that form at specific locations with defined shape and size. Synaptic assembly must be tightly regulated to prevent overgrowth of the synapse size and number, but the molecular mechanisms that inhibit synapse assembly are poorly understood. We identified regulator of synaptogenesis-1 (RSY-1) as an evolutionarily conserved molecule that locally antagonized presynaptic assembly. The loss of RSY-1 in *Caenorhabditis elegans* led to formation of extra synapses and recruitment of excessive synaptic material to presynaptic sites. RSY-1 directly interacted with and negatively regulated SYD-2/liprin- $\alpha$ , a master assembly molecule that recruits numerous synaptic components to presynaptic sites. RSY-1 also bound and regulated SYD-1, a synaptic protein required for proper functioning of SYD-2. Thus, local inhibitory mechanisms govern synapse formation.

Synapse formation is a highly dynamic and regulated process. Although many positive factors that promote synaptogenesis have been identified (1–3), less is known about negative regulators of synapse formation and their mode of action (4–10). We investigated synapse development and its regulation in the hermaphrodite-specific neuron HSNL, one of a pair of motor neurons that controls egg-laying behavior in *Caenorhabditis elegans* (11). Presynaptic specializations in the HSNL neuron assemble within a spatially discrete location along the axon that is stereotyped between animals (Fig. 1, A and B) (12). These presynaptic sites were visualized by transgenically expressing fluorophore-tagged synaptic proteins such as synaptic vesicle component synaptobrevin (SNB-1) or active-zone components ERC/CAST/Bruchpilot (ELKS-1) and GIT-1 (Fig. 1B and fig. S1) (12, 13). SYD-1 and SYD-2 are essential for synapse development in the HSNL neuron; numerous synaptic components failed to localize to presynaptic sites in *syd-1* and *syd-2* mutants (Fig. 1, C and E, and fig. S1) (13, 14). However, increasing SYD-2 function in *syd-1* null mutants, either by overexpressing SYD-2 or by introducing a gain-of-function (gf) mutation in *syd-2*, rescues the synaptic defects observed in *syd-1* mutants (13, 14). Thus, under normal circumstances, SYD-1 is required for SYD-2 function. The existence of such positive regulators suggests that negative regulators of SYD-2 might counteract and balance the pro-synaptic function of SYD-1.

To isolate putative negative regulators of synaptogenesis, we performed a visual genetic screen for mutants that suppress the synaptic defects in the HSNL of *syd-1* mutants (15). We recovered

two alleles of regulator of synaptogenesis-1 (*rsy-1*). In *syd-1;rsy-1* double mutants, the accumulation of SNB-1::yellow fluorescent protein (YFP) in the synaptic region of the HSNL was significantly higher than in *syd-1* single mutants (Fig. 1, C to E). The accumulation of SNB-1::YFP in these double mutants probably represents a restoration of functional synapses. First, active-zone components ELKS-1 and GIT-1 also localized at higher levels to presynaptic sites in *rsy-1;syd-1* double mutants than in *syd-1* single mutants (fig. S1). Second, defects in the egg-laying behavior in *syd-1* mutants, which are a cell-autonomous consequence of the presynaptic assembly defects in the HSNL neuron, were rescued in *rsy-1;syd-1* double mutants (Fig. 1F). Thus RSY-1 appears to counteract and balance the pro-synaptic function of SYD-1.

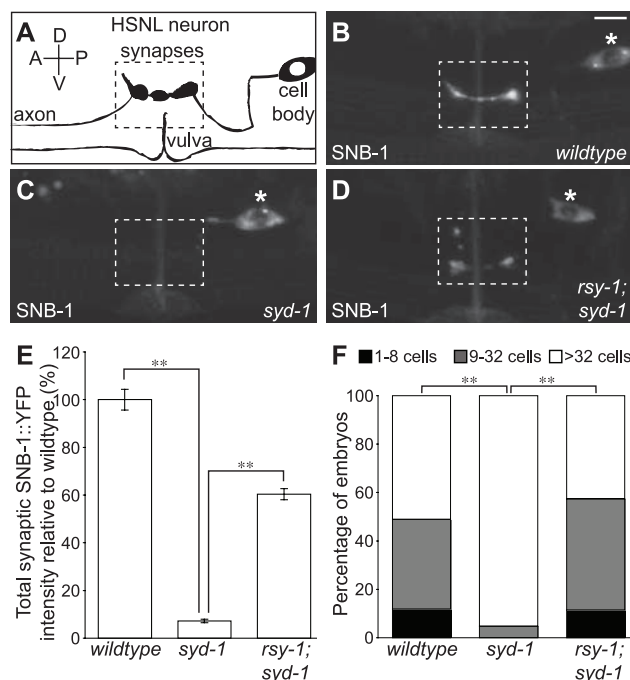
We mapped *rsy-1* to the genetic locus Y53H1A.1, which encodes two isoforms. Iso-

form A encodes a 589–amino acid protein with a proline-rich region, a coiled-coil domain, and a serine/arginine-rich (SR) domain (fig. S2). The SR domain of RSY-1 contains multiple putative nuclear localization sequences (NLSs). Isoform B encodes a smaller 517–amino acid protein that lacks the SR domain, which is replaced by 22 amino acids with a single putative NLS that is unique to the B isoform (fig. S2). RSY-1 is well conserved in vertebrates with both a long and a short isoform in *Mus musculus* (fig. S2). The vertebrate homolog of RSY-1 interacts with pinin (16), a dual resident of the nucleus and the desmosome junction with proposed functions including cell adhesion, transcription, and splicing (17–20). Beyond its interaction with pinin, no function has yet been assigned to RSY-1.

Both alleles of *rsy-1* that we isolated contained mutations that generate early stop codons, suggesting that they are likely to be null alleles (fig. S2). To determine where *rsy-1* is expressed, we made transgenic animals with a synthetic operon in which expression of both RSY-1 and cytoplasmic green fluorescent protein (GFP) is under control of the *rsy-1* promoter (fig. S3). RSY-1 was reproducibly expressed in the HSNL (Fig. 2A), as well as in other neurons and tissues (fig. S4). To determine whether RSY-1 functions cell-autonomously in the HSNL, we transgenically expressed isoform A of RSY-1 under the control of the *unc-86* promoter, which only expresses in the HSNs in the vulva region (21). Expression of the *Punc-86::rsy-1* transgene in *rsy-1;syd-1* double mutants restored synaptic defects in the HSNL of *syd-1* single mutants (Fig. 2B and fig. S5), consistent with a cell-autonomous role for RSY-1 in inhibiting presynaptic assembly.

Next, we sought to determine the subcellular localization of RSY-1. GFP-tagged RSY-1 (iso-

**Fig. 1.** RSY-1 antagonizes the pro-synaptic function of SYD-1. (A) Schematic of the HSNL neuron. Synapses are shown in the dotted rectangle. Anterior, A; posterior, P; dorsal, D; ventral, V. (B) SNB-1::YFP is expressed in the HSNL in *wildtype(N2)*, (C) *syd-1(ju82)*, and (D) *rsy-1(wy94);syd-1(ju82)* mutants. All images are of adults. The dotted rectangle indicates the synaptic region, and the asterisk marks the HSNL cell body. Scale bar, 5  $\mu$ m. (E) Total SNB-1::YFP intensity at the synaptic region normalized to wild type. **\*\*** $P < 0.01$ ; Student's *t* test;  $n > 20$  per group. Error bars indicate SEM. (F) Proportion of eggs at a particular stage when laid. Scored double blind. **\*\*** $P < 0.01$ ; Fisher's exact test;  $n > 20$  per group.



<sup>1</sup>Neurosciences Program, Stanford University, 385 Serra Mall, Herrin Labs, Room 144, Stanford University, Stanford, CA 94305, USA. <sup>2</sup>Howard Hughes Medical Institute, Stanford University, Stanford, CA 94305, USA. <sup>3</sup>Departments of Biology and Pathology, 385 Serra Mall, Herrin Labs, Room 144, Stanford University, Stanford, CA 94305, USA.

\*To whom correspondence should be addressed. E-mail: kangshen@stanford.edu

form A) expressed in the HSNL localized to presynaptic sites as well as to the nucleus (Fig. 2C and fig. S6). Because both isoforms of RSY-1 contain putative NLSs at the C terminus, we used a truncated version of RSY-1 (RSY-1ΔSR) that

lacks all putative NLSs to determine whether the synaptic function of RSY-1 requires its localization to the nucleus. When expressed in the HSNL of *rsy-1;syd-1* double mutants, RSY-1ΔSR completely restored the reduction of SNB-1::YFP

accumulation at presynaptic sites to levels observed in *syd-1* mutants (Fig. 2B). Furthermore, GFP-tagged RSY-1ΔSR was mostly excluded from the HSNL nucleus but robustly localized to the presynaptic sites, where it colocalized with RAB-3, a synaptic vesicle marker (Fig. 2D and fig. S6). Thus, localization of RSY-1 at the presynaptic sites (but not in the nucleus) is probably important for its function in inhibiting synaptogenesis.

To further characterize presynaptic localization of RSY-1, we examined RSY-1ΔSR localization in *unc-104* mutants. UNC-104 is an ortholog of the vertebrate Kif1A, a kinesin motor essential for trafficking of synaptic vesicles (22). RSY-1ΔSR localization to presynaptic sites was not affected in *unc-104* mutants (Fig. 2E), suggesting that RSY-1 is not associated with synaptic vesicles. Furthermore, RSY-1ΔSR tightly colocalized with active-zone component SYD-2 (fig. S7). RSY-1ΔSR also colocalized with synaptic protein GIT-1 and was juxtaposed to another active-zone protein, ELKS-1 (fig. S8). Thus, RSY-1 occupies a particular subdomain of the active zone and locally regulates synapse assembly.

To determine when RSY-1 acts during the synaptic maturation process, we examined the localization of RSY-1ΔSR at nascent synapses of HSNL in the early and mid-L4 stages of development (12). RSY-1 accumulated at the developing presynaptic sites in early and mid-L4 stages concomitantly with RAB-3 (fig. S9), suggesting that RSY-1 could regulate synaptogenesis from the very early stages of synapse development. Future localization study of endogenous RSY-1 protein will probably provide additional information.

If RSY-1 is a negative regulator of synapse formation, then *rsy-1* single mutants should have elevated synaptogenic activity. SNB-1::YFP levels at presynaptic sites in the HSNL were increased in *rsy-1* mutants (Fig. 3, A, B, and I), suggesting that excessive synaptic material is recruited to the presynaptic sites. During development, synapses form at secondary sites outside of the normal synaptic region of the HSNL, which are then gradually eliminated as animals reach adulthood (8). Elimination of these synapses is partially dependent on proteasomal degradation (8). We observed a partial failure in the elimination of SNB-1::YFP localized to these secondary sites in *rsy-1* mutants (Fig. 3, A to D). These SNB-1::YFP accumulations probably represent presynaptic specializations because RAB-3 colocalized with the active-zone components ELKS-1 and GIT-1 at these sites (fig. S10). The persistence of synapses at secondary sites in *rsy-1* mutants suggests that local inhibition of presynaptic assembly by RSY-1 also contributes to the elimination of synapses. Thus, RSY-1 plays a role in controlling the size and number of presynaptic sites.

RSY-1 can inhibit synaptogenesis by either negatively regulating SYD-2 function or antagonizing

**Fig. 2.** Molecular characterization of *rsy-1*. (A) *rsy-1::sl2::gfp* expressed under the *rsy-1* promoter, which consists of 580 base pairs upstream of the *rsy-1* start site. (B) Total SNB-1::YFP intensity at the synaptic region normalized to wild type. *Punc-86::rsy-1* and *Punc-86::rsy-1ΔSR* denote transgenic expression of *rsy-1* or *rsy-1ΔSR* cDNA (isoform A), respectively. \*\**P* < 0.01; Student's *t* test; *n* > 20. Error bars indicate SEM. (C) GFP::RSY-1 (isoform A) expressed in the HSNL under the *unc-86* promoter. (D) GFP::RSY-1ΔSR (RSY-1 without amino acids 503 to 589 of isoform A) (in green) and mCherry::RAB-3 (in magenta) coexpressed in the HSNL in wild-type (*N2*) and (E) in *unc-104(e1265)* mutants. Insets in the lower left-hand corner in (D) and (E) show GFP::RSY-1ΔSR (green) alone, and insets in the lower right-hand corner show mcherry::RAB-3 (magenta) alone. All images are of adults. The dotted rectangle indicates the synaptic region, and the asterisk marks the HSNL cell body. Scale bar, 5 μm.

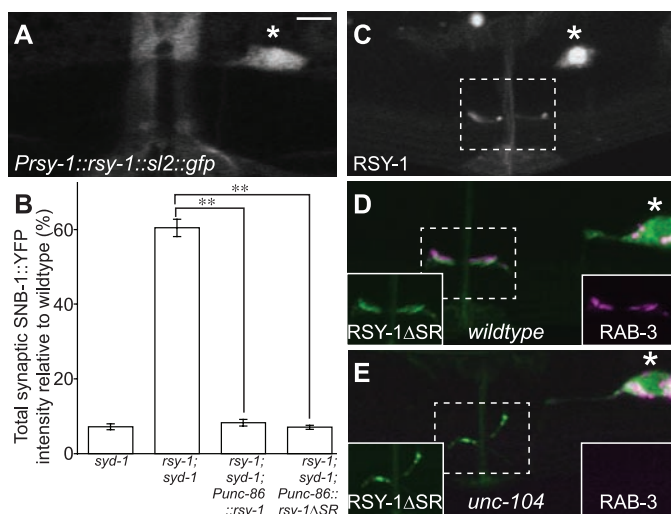
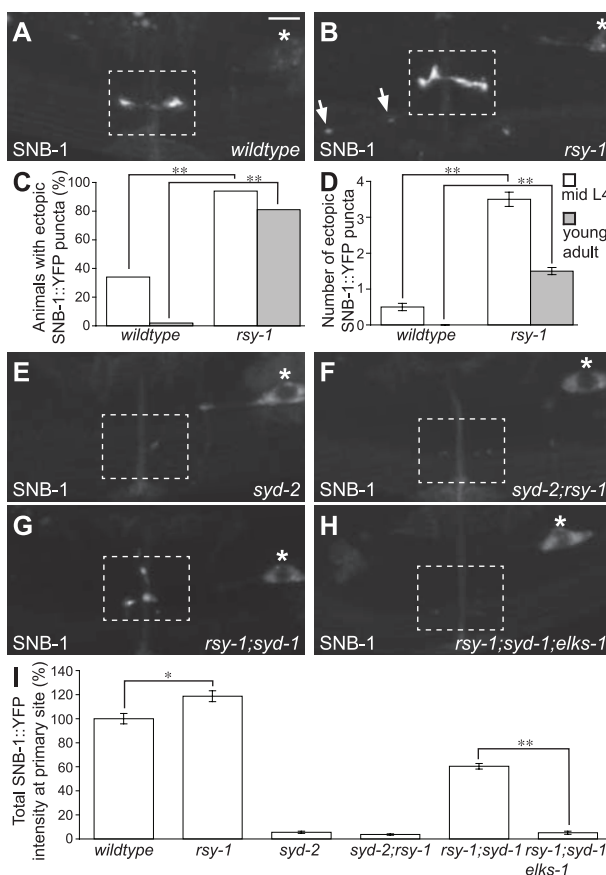


**Fig. 3.** RSY-1 is a negative regulator of SYD-2-dependent synapse assembly. (A) SNB-1::YFP expressed in the HSNL *wildtype(N2)* and (B) *rsy-1(wy94)* mutants. Arrows denote ectopic SNB-1::YFP puncta. (C) Percentage of animals with ectopic SNB-1::YFP puncta in *wildtype(N2)* and *rsy-1(wy94)* mutants at mid-L4 and young adult stages. \*\**P* < 0.01; Fisher's exact test; *n* = 100 per group. (D) Average number of ectopic SNB-1::YFP puncta in *wildtype(N2)* and *rsy-1(wy94)* mutants at mid-L4 and young adult stages. \*\**P* < 0.01; Student's *t* test; *n* = 100 per group. Error bars indicate SEM. (E) SNB-1::YFP accumulation at synapses in *syd-2(ju37)*, (F) *syd-2(ju37);rsy-1(wy94)*, (G) *rsy-1(wy94);syd-1(ju82)*, and (H) *rsy-1(wy94);syd-1(ju82);elks-1(tm1233)* mutants. All images are of adults. The dotted rectangle indicates the synaptic region, and the asterisk marks the HSNL cell body. Scale bar, 5 μm. (I) Total SNB-1::YFP intensity at the primary synaptic region in the HSNL relative to wild type. \**P* < 0.05; \*\**P* < 0.01; Student's *t* test; *n* > 20 per group. Error bars indicate SEM.



onizing an unknown SYD-2-independent parallel assembly pathway. Similar to *syd-1* suppression, if *rsy-1* mutation is able to suppress synaptic defects in *syd-2* mutants, then the data would be indicative of a model in which RSY-1 functions in parallel with SYD-2. However, we found that *syd-2* is epistatic to *rsy-1*; synaptic defects in *syd-2* mutants, as assayed by localization of synaptic proteins and the egg-laying behavior, were not rescued in *syd-2*;*rsy-1* double mutants (Fig. 3, E, F, and I, and fig. S5). Thus,

RSY-1 probably acts upstream of or in parallel with SYD-2. Both models suggest that RSY-1 is a negative regulator of SYD-2-dependent synapse assembly.

According to the linear model in which *syd-2* acts downstream of *rsy-1*, the function of SYD-2 should increase in *rsy-1* mutants. If this is the case, then the phenotype in *rsy-1* mutants and *syd-2(gf)* animals should be similar. Indeed, more synaptic material was recruited to presynaptic sites in the HSNL in *syd-2(gf)* animals (14), sim-

ilar to our observation in *rsy-1* loss-of-function mutants (Fig. 3I). The linear model also predicts that the rescued synapse assembly in *rsy-1*;*syd-1* mutants, like in *syd-2(gf)*;*syd-1* mutants, is due to an increase in SYD-2 function. If this is the case, then synapses in both double mutants should be similarly susceptible to various genetic manipulations. ELKS-1 is a presynaptic active-zone component shown to be important for the development of presynaptic terminals at the neuromuscular junction in *Drosophila* (23, 24). In *C. elegans*, although the loss of ELKS-1 function by itself does not result in any detectable defects in synapse assembly (13, 14, 25), synapse formation in the HSNL of *syd-2(gf)*;*syd-1* mutants is crucially dependent on ELKS-1 (14). Thus, ELKS-1 functions redundantly with SYD-1 to promote synapse assembly. Synapse formation in *rsy-1*;*syd-1* double mutants was also dependent on *elks-1* (Fig. 3, G to I, and fig. S5). Thus, the synapse assembly program deployed in *rsy-1*;*syd-1* mutants is similar to the one in *syd-2(gf)*;*syd-1* mutants. In summary, the loss of RSY-1 function has similar consequences as the gain of SYD-2 function. Although these results do not rule out the possibility that RSY-1 functions in parallel with SYD-2, given that RSY-1 interacts with SYD-2 as described below, they are consistent with a genetic model in which RSY-1 is a negative regulator of SYD-2.

RSY-1 could interfere with the pro-synaptic function of SYD-2 directly or inhibit the function of SYD-2 indirectly by blocking SYD-1. To test these possibilities, we used a single-cell in situ protein-protein interaction assay (26, 27), in which translocation of the prey to the plasma membrane is tested in the presence of a membrane-tethered bait, to determine whether RSY-1 physically interacts with SYD-2 and SYD-1. RSY-1ΔSR bound to both SYD-2 [via the first two SAM domains] and SYD-1 (note the enrichment of SYD-2SAMI-2 and SYD-1 on the plasma membrane in the presence of membrane-targeted RSY-1ΔSR) (Fig. 4, A, B, and G). Furthermore, coimmunoprecipitation from worm lysates confirmed that RSY-1ΔSR interacted with both SYD-2 and SYD-1 in vivo (fig. S11).

To study the molecular consequence of interaction of RSY-1 with SYD-2 and SYD-1, we first established a readout of SYD-2 function. Vertebrate homologs of ELKS-1 and SYD-2 directly bind in vitro (28), whereas in *C. elegans*, SYD-2 and ELKS-1 coimmunoprecipitate from worm lysate (14). Furthermore, *syd-2* loss-of-function analysis suggests that SYD-2 is necessary for localizing ELKS-1 to presynaptic sites, whereas experiments with the *syd-2(gf)* allele suggest that SYD-2 is sufficient for recruiting ELKS-1 (13, 14). Given these data and the genetic evidence that ELKS-1 is an important component of the presynaptic assembly program, we used the ELKS-1/SYD-2 interaction as one of the readouts of SYD-2 function.

Although there was little detectable interaction between ELKS-1 and SYD-2 in our assay,

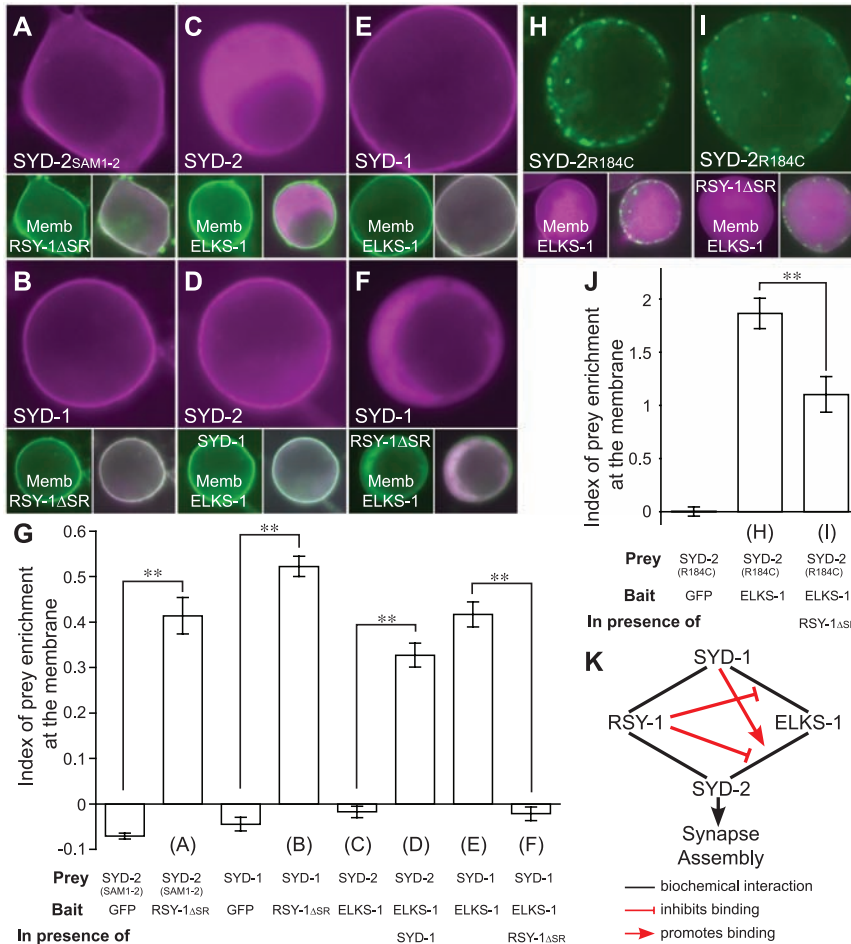


**Fig. 4. Molecular mechanisms of RSY-1 function. (A)** mCherry::SYD-2SAMI-2 (amino acids 853 to 1085 of SYD-2) (magenta, main panel) coexpressed in Hek293T cells with membrane-targeted GFP::RSY-1ΔSR (green, lower left panel; lower right panel shows a merged image). **(B)** mCherry::SYD-1 coexpressed with membrane-targeted GFP::RSY-1ΔSR. **(C)** mCherry::SYD-2 coexpressed with membrane-targeted GFP::ELKS-1 in the absence of and **(D)** in the presence of cytoplasmic GFP::SYD-1. **(E)** mCherry::SYD-1 coexpressed with membrane-targeted GFP::ELKS-1 in the absence of and **(F)** in the presence of cytoplasmic GFP::RSY-1ΔSR. **(G)** Quantification of prey translocation to the plasma membrane. **(H)** eYFP::SYD-2R184C (arginine amino acid at position 184 switched to cysteine) (green, main panel) coexpressed with membrane-targeted mCherry::ELKS-1 (magenta, lower left panel; lower right panel shows a merged image) in the absence of and **(I)** in the presence of cytoplasmic mCherry::RSY-1ΔSR. **(J)** Quantification of prey translocation to the plasma membrane. In **(G)** and **(J)**, the index of prey enrichment at the membrane was calculated by the following expression: (prey fluorescence intensity at the cell membrane/cytoplasm) – 1. An index of 0 indicates equal fluorescence intensity at the membrane and in the cytoplasm. \*\**P* < 0.01; Student's *t* test; *n* = 15 per group. Error bars indicate SEM. Letters corresponding to figure panels are shown below the appropriate bar. The prey, membrane-targeted bait, and third cytoplasmic protein present are indicated below each bar. **(K)** Summary of biochemical interactions and their consequences. Promotion of SYD-2/ELKS-1 interaction by SYD-1 supports the genetic data that *syd-1* is normally required for *syd-2* function. Inhibition of SYD-2/ELKS-1 and SYD-1/ELKS-1 interaction by RSY-1 supports the genetic role of *rsy-1* in antagonizing *syd-2* directly and indirectly via *syd-1*.

the interaction was greatly enhanced in the presence of SYD-1 (Fig. 4, C, D, and G), suggesting that SYD-1 facilitates binding between ELKS-1 and SYD-2. Consistent with this result, SYD-1 directly interacted with ELKS-1 (Fig. 4, E and G), and this interaction was weakened in the presence of RSY-1ΔSR (Fig. 4, F and G). Thus, one way in which RSY-1 regulates SYD-2 function is indirectly by weakening the interaction of SYD-1 with ELKS-1 and thus potentially blocking the ability of SYD-1 to facilitate SYD-2 function (Fig. 4K).

Given that the ELKS-1/SYD-2 binding is very weak in the absence of SYD-1 in our assay, we could not test whether interaction of RSY-1 with SYD-2 inhibited ELKS-1/SYD-2 binding. However, the ELKS-1/SYD-2 interaction does increase when SYD-2 contains a gain-of-function mutation, Arg<sup>184</sup> → Cys<sup>184</sup> (R184C) (14), which was verified in our cell-based assay (Fig. 4, H and J). We then tested the effect of RSY-1 on this interaction and found that the interaction between ELKS-1 and SYD-2R184C was weakened in the presence of RSY-1ΔSR (Fig. 4, I and J), suggesting that, besides acting via SYD-1, RSY-1 can also directly antagonize the ability of SYD-2 to recruit ELKS-1 (Fig. 4K).

It is increasingly clear that positive and negative regulators control synapse development at multiple levels. For example, the transcription factor MEF2 globally regulates the number of excitatory synapses (7). Three ubiquitin ligase complexes also regulate presynaptic development (5, 8, 29). Here, RSY-1 was shown to act as a negative regulator of synaptogenesis by coun-

teracting SYD-1 function to inhibit SYD-2-dependent presynaptic assembly in the HSNL neuron. RSY-1 controls the amount of synaptic material recruited to presynaptic sites. RSY-1 also plays a role in establishing a balance between synapse formation and synapse elimination. RSY-1 achieves these functions by interacting with integral components of the synapse assembly machinery and by regulating a dense network of protein-protein interactions between various active-zone molecules (Fig. 4K).

#### References and Notes

- M. Zhen, Y. Jin, *Nature* **401**, 371 (1999).
- M. Zhen, Y. Jin, *Curr. Opin. Neurobiol.* **14**, 280 (2004).
- C. L. Waites, A. M. Craig, C. C. Garner, *Annu. Rev. Neurosci.* **28**, 251 (2005).
- Q. Chang, R. J. Balice-Gordon, *Neuron* **26**, 287 (2000).
- P. van Roessel, D. A. Elliott, I. M. Robinson, A. Prokop, A. H. Brand, *Cell* **119**, 707 (2004).
- K. Nakata *et al.*, *Cell* **120**, 407 (2005).
- S. W. Flavell *et al.*, *Science* **311**, 1008 (2006).
- M. Ding, D. Chao, G. Wang, K. Shen, *Science* **317**, 947 (2007); published online 11 July 2007 (10.1126/science.1145727).
- M. P. Klassen, K. Shen, *Cell* **130**, 704 (2007).
- V. Y. Poon, M. P. Klassen, K. Shen, *Nature* **455**, 669 (2008).
- C. Desai, H. R. Horvitz, *Genetics* **121**, 703 (1989).
- K. Shen, C. I. Bargmann, *Cell* **112**, 619 (2003).
- M. R. Patel *et al.*, *Nat. Neurosci.* **9**, 1488 (2006).
- Y. Dai *et al.*, *Nat. Neurosci.* **9**, 1479 (2006).
- Materials and methods are available as supporting material on Science Online.
- G. Zimowska *et al.*, *Invest. Ophthalmol. Vis. Sci.* **44**, 4715 (2003).
- P. Ouyang, *Biochem. Biophys. Res. Commun.* **263**, 192 (1999).
- J. H. Joo *et al.*, *Mol. Vis.* **11**, 133 (2005).
- R. Alpatov *et al.*, *Mol. Cell. Biol.* **24**, 10223 (2004).

- P. Wang, P. J. Lou, S. Leu, P. Ouyang, *Biochem. Biophys. Res. Commun.* **294**, 448 (2002).
- R. Baumeister, Y. Liu, G. Ruvkun, *Genes Dev.* **10**, 1395 (1996).
- D. H. Hall, E. M. Hedgecock, *Cell* **65**, 837 (1991).
- D. A. Wagh *et al.*, *Neuron* **49**, 833 (2006).
- R. J. Kittel *et al.*, *Science* **312**, 1051 (2006); published online 13 April 2006 (10.1126/science.1126308).
- S. L. Deken *et al.*, *J. Neurosci.* **25**, 5975 (2005).
- D. Blanchard, H. Hutter, J. Fleenor, A. Fire, *Mol. Cell. Proteomics* **5**, 2175 (2006).
- M. D. Muzumdar, B. Tasic, K. Miyamichi, L. Li, L. Luo, *Genesis* **45**, 593 (2007).
- J. Ko, M. Na, S. Kim, J. R. Lee, E. Kim, *J. Biol. Chem.* **278**, 42377 (2003).
- T. A. Fulga, D. Van Vactor, *Neuron* **57**, 339 (2008).
- We would like to thank the *Caenorhabditis* Genetics Center and the Japanese NBPR for strains; Y. Kohara (National Institute of Genetics, Japan) for Y53H1A.1 cDNAs; J. Audhya (University of California, San Diego) for *C. elegans* optimized mCherry cDNA; L. Luo (Stanford University) for vertebrate mCherry cDNA; T. Meyer (Stanford University) for eYFP-C3 plasmid; M. Park (Stanford University) for mCerulean-C1 plasmid; C. Gao for technical assistance; and members of the Shen lab, C. Bargmann, T. Clandinin, and L. Luo for critical comments on the manuscript. We would also like to thank B. Grill (Stanford University) for providing protocol and guidance for coimmunoprecipitation experiments. This work was funded by grants awarded to K.S. [from NIH (1R01NS048392), the Human Frontier Science Foundation, the Howard Hughes Medical Institute, and the W. M. Keck Foundation] and by a National Research Service Award predoctoral fellowship awarded to M.R.P. by NIH.

#### Supporting Online Material

www.sciencemag.org/cgi/content/full/323/5920/1500/DC1  
Materials and Methods

Figs. S1 to S11  
References

26 November 2008; accepted 7 January 2009  
10.1126/science.1169025

## The Role of Fingerprints in the Coding of Tactile Information Probed with a Biomimetic Sensor

J. Scheibert,\* S. Leurent, A. Prevost,† G. Debrégeas‡

In humans, the tactile perception of fine textures (spatial scale <200 micrometers) is mediated by skin vibrations generated as the finger scans the surface. To establish the relationship between texture characteristics and subcutaneous vibrations, a biomimetic tactile sensor has been designed whose dimensions match those of the fingertip. When the sensor surface is patterned with parallel ridges mimicking the fingerprints, the spectrum of vibrations elicited by randomly textured substrates is dominated by one frequency set by the ratio of the scanning speed to the interridge distance. For human touch, this frequency falls within the optimal range of sensitivity of Pacinian afferents, which mediate the coding of fine textures. Thus, fingerprints may perform spectral selection and amplification of tactile information that facilitate its processing by specific mechanoreceptors.

The hand is an important means for human interaction with the physical environment (1). Many of the tasks that the hand can undertake—such as precision grasping and manipulation of objects, detection of individual defects on smooth surfaces, and discrimination of textures—depend on the exquisite tactile sensi-

tivity of the fingertips. Tactile information is conveyed by populations of mechanosensitive afferent fibers innervating the distal fingerpads (2, 3). In recent years, a breakthrough in our understanding of the coding of roughness perception has been made with the experimental confirmation of Katz's historical proposition of the ex-

istence of two independent coding channels that are specific for the perception of coarse and fine textures (4–6). The perception of coarse textures (with features of lateral dimensions larger than about 200 μm) relies on spatial variations of the finger/substrate contact stress field and is mediated by the slowly adapting mechanoreceptors (7). The perception of finer textures (<200 μm) requires the finger to be scanned across the surface because it is based on the cutaneous vibrations thus elicited. These vibrations are intensively encoded, principally by Pacinian fibers (8), which are characterized by a band-pass behavior with a best frequency (i.e., the stimulus frequency where maximum sensitivity occurs) on the order of 250 Hz (9). The most elaborated description of the latter coding scheme was given by Bensmaïa and Hollins, who directly measured the skin vibrations of fingers scanning finely tex-

Laboratoire de Physique Statistique de l'École Normale Supérieure, CNRS UMR 8550, Associé aux Universités Paris 6 et Paris 7, 24 rue Lhomond, 75231 Paris Cedex 05, France.

\*Present address: Physics of Geological Processes, University of Oslo, Post Office Box 1048 Blindern, N-0316 Oslo, Norway.

†Present address: Laboratoire de Physique Théorique, 24 rue Lhomond, 75231 Paris Cedex 05, France.

‡To whom correspondence should be addressed. E-mail: georges.debrégeas@lps.ens.fr.